Buenos Aires – 5 to 9 September, 2016
Acoustics for the 21st Century…

PROCEEDINGS of the 22nd International Congress on Acoustics

Biomedical Acoustics: Paper ICA2016-643

Sensitivity of high-frequency ultrasound to breast cancer lobular carcinomas: results from phantom and surgical specimen studies

Nicole Cowan[(a)], Zachary Coffman[(a)], Robyn Omer[(a)], Timothy Doyle[(a)]

[(a)] Utah Valley University, United States, timothy.doyle@uvu.edu

Abstract

A majority of women with early stage breast cancer select breast conservation surgery (BCS) over mastectomy. A key issue with BCS, however, is the high percentage of patients (30-60%) who require additional surgery to remove residual cancer that was not identified during the initial operation. This is especially true for patients with lobular carcinomas since they are difficult to detect. At Utah Valley University, a high-frequency (HF) ultrasonic method has shown promise as a rapid, intraoperative method for detecting residual breast cancer in surgical margins. The objective of this project was to determine the sensitivity of HF ultrasound to lobular carcinoma using histology mimicking phantoms and surgical margins. Phantoms were created from distilled water, agarose powder, 10X TBE stock solution, and polyethylene microspheres (98-μm dia.) and fibers (35-μm dia.) to simulate breast tissue histology. Three experiments were conducted with specimens containing only microspheres (E1), only fibers (E2), and a mixture of both (E3) to more accurately model breast tissue histology. Microsphere and fiber weight percents were varied for each specimen. Pitch-catch measurements were acquired using 50-MHz transducers, a HF ultrasound system, and glycerol as the coupling agent. Attenuation showed definite trends for E1 and E3, but no trend for E2. Peak density showed no trend for any of the experiments. HF ultrasonic tests on margin specimens from two studies performed at the Huntsman Cancer Institute (90 patients total) showed that both attenuation and peak density were most sensitive to lobular carcinomas. Both phantom and surgical margin results indicate that HF ultrasound shows a higher sensitivity to lobular carcinoma histologies as compared to ductal carcinoma histologies.

Keywords: High-frequency ultrasound, breast cancer, margins

Sensitivity of high-frequency ultrasound to breast cancer lobular carcinomas: results from phantom and surgical specimen studies

1 Introduction

Determining the pathology of soft tissues non-invasively and in real time would benefit several medical procedures including screening, endoscopy, and biopsy as well as exploratory and surgical procedures. In particular, the use of such a method for the intraoperative assessment of margins in breast conservation surgery (BCS) would significantly improve the quality of care for breast cancer patients. Obtaining negative (cancer free) margins in BCS is critical for local control of cancer in the affected breast, and failure to obtain negative margins during BCS results in additional surgery for 30-60% of patients [1-6]. A number of methods are therefore being investigated for the intraoperative evaluation of margin status, including small specimen radiography, radio-frequency spectroscopy, optical methods, and terahertz wave methods [7-12].

Invasive lobular carcinoma (ILC) comprises 5-15% of breast cancers, and is more difficult to detect radiographically than ductal carcinomas due to its diffuse growth characteristics [13]. ILC typically infiltrates tissue in single-cell wide filaments dispersed through the stroma. Diagnostic imaging methods, therefore, show lower sensitivities for ILC as compared to ductal carcinomas, including mammography, ultrasound, and magnetic resonance imaging (79%, 68%, and 83% sensitivities, respectively) [14]. Negative margins are particularly difficult to achieve for ILC, with six studies reporting 49-63% positive or close margins following the initial surgery, and one study reporting 39% positive or close margins with the use of full thickness excision and oncoplastic surgery [15]. Many patients with ILC therefore end up receiving multiple (three or more) surgeries and often a mastectomy due to the inability to obtain negative margins.

Ultrasonic wave propagation in tissues strongly depends on histological features including cell structure, cell number density, tissue microstructure, and tissue heterogeneity [16]. Ultrasound therefore has the potential to differentiate between normal, benign, and malignant pathologies in breast tissue [17]. For example, Jeong *et al.* (2008) used 2-10 MHz ultrasonic tomography to map regions in eight mastectomy specimens into three tissue types: Normal, benign changes, and invasive carcinoma [18]. The use of frequency dependent attenuation and high resolution scans ($\leq$ 1 mm) provided a significant degree of correlation to histopathology, yielding an 80% sensitivity, 90% specificity, and 86% accuracy. High-frequency (HF) ultrasound has been used to detect histological changes associated with mammary tumors in mice at 10-25 MHz [19], to differentiate normal and malignant human breast epithelial cells in monolayer cell cultures at 20-50 MHz [20], to determine tumor size and margin status in 2-5 mm thick slices of ductal carcinoma tissue with scanning acoustic microscopy at 15-50 MHz [21], and in mouse tumors following photodynamic and radiation therapies [22,23].

The objective of this study was to investigate the sensitivity of HF ultrasound in the 20-80 MHz range to lobular carcinomas in margin surgical specimens. Histology mimicking phantoms were

constructed with fibrous and spherical inclusions to simulate ductal and lobular microstructures, and were tested with HF ultrasound. The sensitivity of the ultrasound to inclusion type, size, and concentration was compared. Finally, the results were compared to those from a 17-patient pilot study of HF ultrasound on BCS surgical specimens [24]. This pilot study, performed at the Huntsman Cancer Institute in Salt Lake City, Utah, demonstrated a high sensitivity to lobular carcinomas as compared to benign tissue and ductal carcinomas. The goal of this study was to validate the pilot study results with corroborating phantom data.

2 Methods

2.1 Phantoms

Four experiments were conducted with histology mimicking breast tissue phantoms: E1, E2, E3, and E4. Breast tissue phantoms were created using 10X TBE Solution, distilled water, and agarose powder to create 3% agarose phantoms by concentration. Agarose was used as the phantom medium as a result of its well-characterized performance, the ease of fabrication, and the flexibility to incorporate additional ingredients to achieve a range of target acoustic properties [25]. Polyethylene microspheres (Cospheric, 58-550 µm diameter) and/or microfibers (Mini Fibers, Inc., 35 µm diameter, 6.35 mm length) were added to the phantoms in layers to eliminate the production of air bubbles and ensure proper distribution of the inclusions within the phantoms. A first layer of agarose was poured into a molding tray and polyethylene inclusions were gently mixed into the layer until evenly distributed. In order to not disturb the previous layer, the base layers were allowed to cool and solidify before consecutive layers were added. Upon solidification, a successive layer of agarose with inclusions was carefully added. This process was continued for following layers before a final layer of agarose, without inclusions, was added to act as a coupling layer. Three phantoms of 3% agarose, equivalent thickness, and without inclusions were also produced as controls for each experiment.

In experiment E1, polyethylene microspheres (90-106 µm) were added to the phantoms in 4-mm thick layers. Total thickness for each phantom was approximately 20 mm. Microspheres were measured into six increment weights ranging from 10-60 mg to produce six phantoms that simulated a range of breast tissue densities. Each increment weight was divided into four equal portions for inclusion into the phantoms (each portion for each boundary between agarose layers). An image of the completed phantoms can be seen in Figure 1a.

In experiment E2, microfibers were added to the phantoms in 2-mm thick layers. In E2, each phantom totaled approximately 6-9 mm thick to more closely match the surgical specimens. The microfibers were measured into six increment weights (10-60 mg) to produce six phantoms that simulated a range of breast tissue densities. The microfibers were divided into two equal portions for inclusion into the phantoms. A thin 2-mm layer of agarose was poured into a molding tray and allowed to solidify. Upon solidification the microfibers were evenly distributed across the top of the layer utilizing a fine-tipped paint brush, which prevented clumping and allowed fiber separation and dispersion. A consecutive, equally thick layer of agarose and microfiber inclusions was added following the same process. A final layer of agarose without

microfiber inclusions was then added to the phantom to act as a coupling layer. Three 8-mm phantoms of 3% agarose without microfibers were made as controls.

In experiment E3, a combination of both polyethylene microspheres (90-106 μm) and microfibers were used to more accurately mimic the fibrous and glandular tissues of the breast. The microspheres (5-30 mg) and microfibers (10-60 mg) were measured into six increment weights to produce six phantoms that simulated a range of breast tissue densities. Each weight increment was divided into equal parts for inclusion in the phantoms. The same process described in experiment E2 was utilized for phantom fabrication in this experiment. Three 8-mm thick phantoms of 3% agarose without inclusions were made as controls. A photomicrograph of a completed phantom is shown in Figure 1b. In experiment E4, phantoms were made with equal weight percent of microspheres (0.8%), but with varying microsphere diameter (58-550 μm).

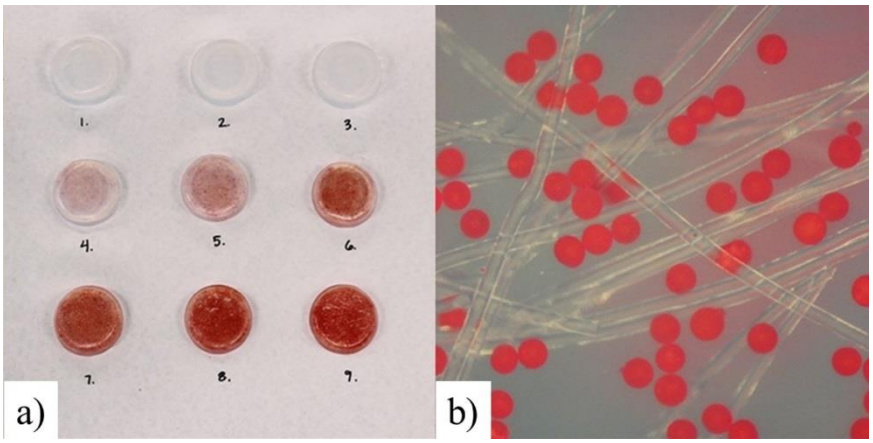

Figure 1: (a) Phantoms from experiment E1. (b) Micrograph of phantom from experiment E3.

2.2 Ultrasound Testing

Pitch-catch (through-transmission) measurements were acquired from the phantom specimens with the use of a HF ultrasound system equivalent to the one used in the 17-patient pilot study. This system consisted of two 50-MHz immersion transducers (Olympus NDT, V358-SU, 12.7-mm OD, 6.35-mm active element diameter), a HF square-wave pulser/receiver (UTEX, UT340), and a 1-GHz digital oscilloscope (Agilent, DSOX3104A). An aluminum test fixture supported the tissue specimen and held the transducers in contact with the sample. Phantoms were tested in a manner similar to surgical specimens. The phantoms were placed inside a resealable plastic bag and positioned on the test fixture. The transducers were acoustically coupled to the outside bag with glycerin. The broadband transducers were driven with a half square wave of 100-volt amplitude and 10-ns width. Ultrasonic waveforms were averaged in the signal acquisition. Triplicate waveforms were collected from multiple positions on each phantom. Specimen thickness was recorded for each measurement.

Parameters measured included peak density, attenuation, and wave velocity. Peak density is the number of peaks (maxima) and valleys (minima) in a specified frequency band of the power spectrum of a HF ultrasound signal. Peak density is a spectral parameter that is obtained from coherent, broadband ultrasonic signals and has been found to correlate with breast tissue

pathology [24]. Peak densities were derived from the time-domain waveforms by performing a Fourier transform and counting the number of peaks and valleys in the 20-80 MHz region of the resulting power spectra. Attenuation and velocity were calculated by scaling the waveforms to account for receiver gain and tissue thickness, and using a Hilbert transform to obtain the waveform envelopes and their corresponding amplitudes and arrival times.

3 Results

3.1 Pilot Study Results

Figure 2 shows the peak density and attenuation results from the BCS surgical specimen study conducted at the Huntsman cancer Institute [24]. The study included 17 patients and 34 specimens. The study showed that peak density most closely matched five broad tissue categories corresponding to (1) fat necrosis, fibroadenomas, and tubular adenomas (FA-FN); (2) normal tissue; (3) benign pathologies including benign calcifications, atypical ductal hyperplasia, fibrocystic changes, and benign papilloma; (4) ductal carcinomas, *in situ* and invasive (DC); and (5) lobular carcinomas, *in situ* and invasive (LC). Attenuation showed less of a correlation to these five pathology categories. However, both peak density and attenuation showed the greatest sensitivity to attenuation.

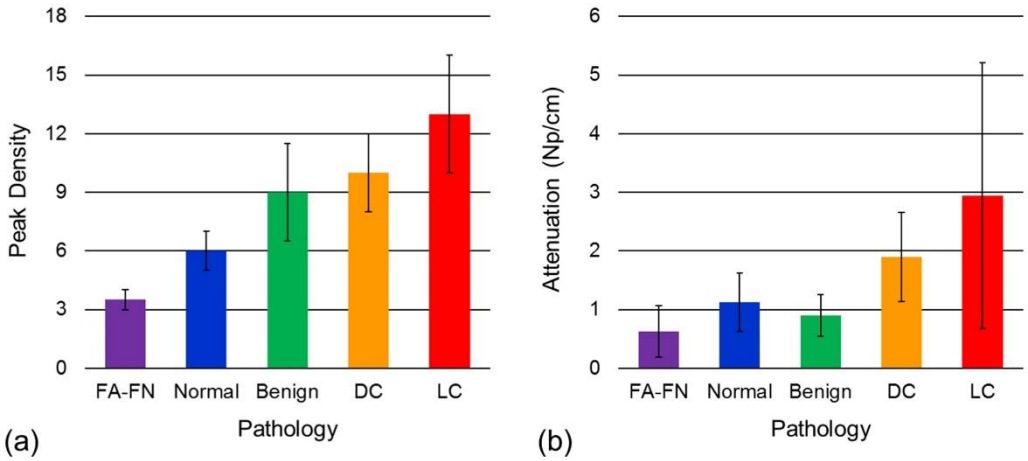

Figure 2: HF ultrasound results from BCS surgical specimen study.

3.2 Phantom Results

Figures 3 and 4 show the HF ultrasound results from experiments E1 and E3, respectively. Both sets of results show that attenuation increases with inclusion concentration, but that peak density does not show any significant trend. Additionally, the attenuation for E1 (microspheres only) shows a greater trend than the attenuation for E3 (microspheres and microfibers). The results indicate that HF ultrasound is more sensitive to spherically shaped microstructures, such as lobules, rather than fiber-shaped structures, such as ductules. The results from experiment E2 support this conclusion, showing no trend for either peak density or attenuation with increasing microfiber concentration.

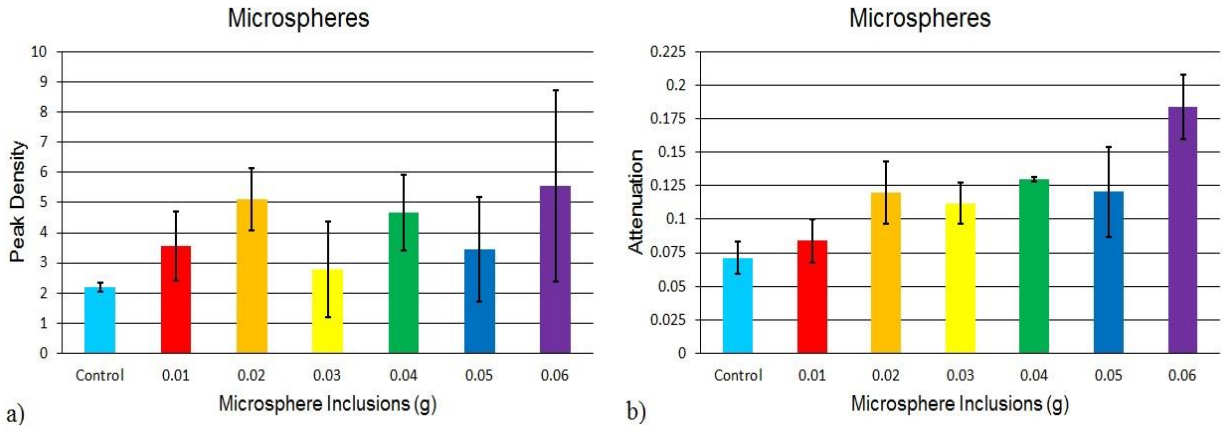

Figure 3: HF ultrasound results from phantom experiment E1.

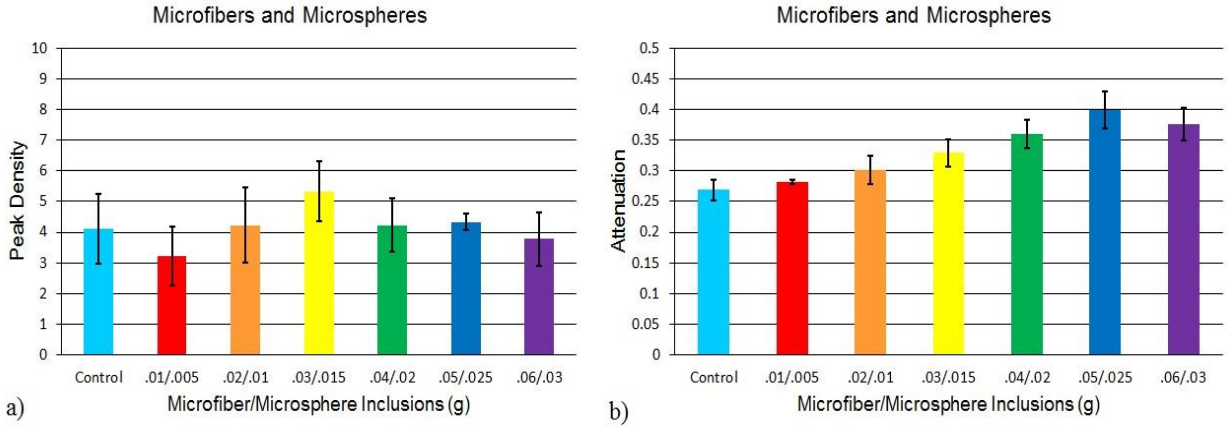

Figure 4: HF ultrasound results from phantom experiment E3.

Figure 5 shows the results from experiment E4, where the microsphere diameters were varied but the total concentration (weight percent) was kept constant. Bars for 0-μm size are controls (no microspheres). The results show that both peak density and attenuation are sensitive to microsphere diameter to different degrees. Peak density exhibits the greatest sensitivity, with a sharp rise for the smallest microspheres (58 and 98 μm). Attenuation displays an almost linear trend with microsphere diameter. In contrast, peak density follows an inverse diameter trend. This inverse diameter trend suggests that peak density's sensitivity to microsphere size is due to a Mie scattering phenomenon, where the scattering becomes significantly more efficient as the microsphere size approaches the wavelength of the ultrasound in the agarose (60 μm for 25 MHz, which is the peak frequency of the ultrasonic waveform after transmission through the phantom).

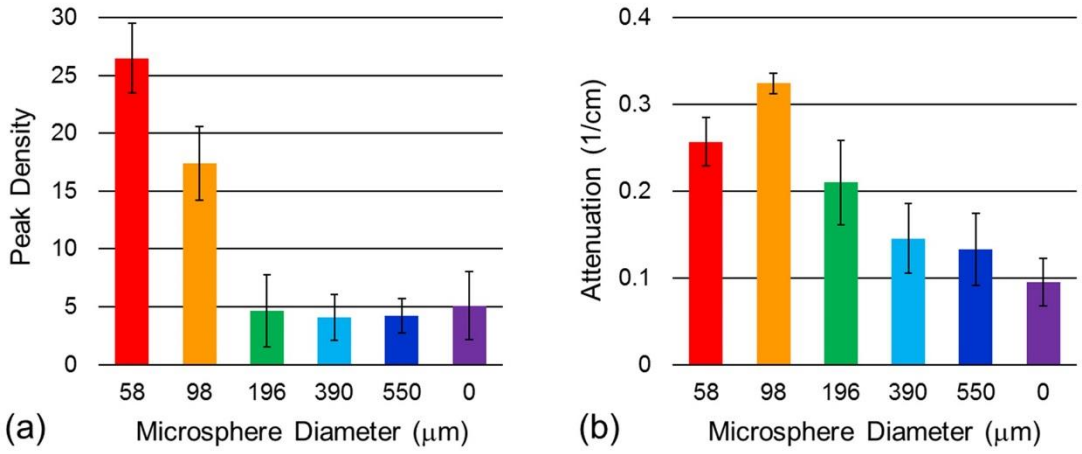

Figure 5: HF ultrasound results from phantom experiment E4.

The results from experiments E1 and E3 (Figures 3 and 4) demonstrate that attenuation is most sensitive to the concentration of spherical (lobular-type) scatterers, whereas the results from experiment E4 demonstrate that peak density is most sensitive to the size of the spherical scatterers at small tissue scales. Most interesting, the results from experiment E2 indicate that both peak density and attenuation are less sensitive to cylindrical (ductule-type) scatterers than they are to spherical (lobular-type) scatterers. These results are consistent with the surgical specimen results shown in Figure 2, where both peak density and attenuation display greater response to lobular carcinomas as compared to ductal carcinomas and benign pathologies.

4 Conclusions

The goal of this study was to explore the comparative sensitivity of high-frequency ultrasound (20-80 MHz) to lobular-type and ductule-type microstructures using histology mimicking phantoms. A 17-patient pilot study on BCS surgical specimens provided preliminary results that the parameters peak density and attenuation were sensitive to lobular carcinomas as compared to ductal carcinomas and benign pathologies such as atypical ductal hyperplasia. The results from four phantom experiments strongly support the results from the pilot study, showing that peak density and attenuation are much more sensitive to lobular-type microstructures (microspheres) than to ductule-type microstructures (microfibers). Future work will include creating and testing phantoms with more histologically accurate microstructures, and comparing the phantom work with a detailed analysis of HF ultrasound results from a 73-patient BCS surgical specimen study recently completed at the Huntsman Cancer Institute.

Acknowledgments

This research was funded by grants from the National Cancer Institute (NIH Award Number R21CA131798), the Western Alliance for Expanding Student Opportunities (Arizona State University), and Utah Valley University.

References

[1] Anscher, M.; Jones, P.; Prosnitz, L.; Blackstock, W.; Hebert, M.; Reddick, R.; Tucker, A.; Dodge, R.; Leight, G.; Iglehart, J.; Rosenman, J. Local failure and margin status in early-stage breast carcinoma treated with conservation surgery and radiation therapy. *Annals of Surgery*, Vol 218 (1), 1993, pp 22-28.

[2] Roukos, D.; Kappas, A.; Agnantis, N. Perspectives and risks of breast-conservation therapy for breast cancer. *Annals of Surgical Oncology*, Vol 10 (7), 2003, pp 718-721.

[3] Moore, M.; Borossa, G.; Imbrie, J.; Fechner, R.; Harvey, J.; Slingluff, C.; Adams, R.; Hanks, J. Association of infiltrating lobular carcinoma with positive surgical margins after breast-conservation therapy. *Annals of Surgery*, Vol 231 (6), 2000, pp 877-882.

[4] Moore, M.; Whitney, L.; Cerilli, L.; Imbrie, J.; Bunch, M.; Simpson, V.; Hanks, J. Intraoperative ultrasound is associated with clear lumpectomy margins for palpable infiltrating ductal breast cancer. *Annals of Surgery*, Vol 233 (6), 2001, pp 761-768.

[5] Cabioglu, N.; Hunt, K.; Sahin, A.; Kuerer, H.; Babiera, G.; Singletary, S.; Whitman, G.; Ross, M.; Ames, F.; Feig, B.; Buchholz, T.; Meric-Bernstam, F. Role for intraoperative margin assessment in patients undergoing breast-conserving surgery. *Annals of Surgical Oncology*, Vol 14 (4), 2007, pp 1458-1471.

[6] Waljee, J.; Hu, E.; Newman, L.; Alderman, A. Predictors of re-excision among women undergoing breast-conserving surgery for cancer. *Annals of Surgical Oncology*, Vol 15 (5), 2008, pp 1297-1303.

[7] Bathla, L.; Harris, A.; Davey, M.; Sharma, P.; Silva, E. High resolution intra-operative two-dimensional specimen mammography and its impact on second operation for re-excision of positive margins at final pathology after breast conservation surgery. *American Journal of Surgery*, Vol 202 (4), 2011, pp 387-394.

[8] Schnabel, F.; Boolbol, S.; Gittleman, M.; Karni, T.; Tafra, L.; Feldman, S.; Police, A.; Friedman, N.; Karlan, S.; Holmes, D.; Willey, S.; Carmon, M.; Fernandez, K.; Akbari, S.; Harness, J.; Guerra, L.; Frazier, T.; Lane, K.; Simmons, R.; Estabrook, A.; Allweis, T. A randomized prospective study of lumpectomy margin assessment with use of MarginProbe in patients with nonpalpable breast malignancies. *Annals of Surgical Oncology*, Vol 21 (5), 2014, pp 1589-1595.

[9] Kennedy, S.; Geradts, J.; Bydlon, T.; Brown, J.; Gallagher, J.; Junker, M.; Barry, W.; Ramanujam, N.; Wilke, L. Optical breast cancer margin assessment: an observational study of the effects of tissue heterogeneity on optical contrast. *Breast Cancer Research*, Vol 12, 2010, pp R91.

[10] Haka, A.; Volynskaya, Z.; Gardecki, J.; Nazemi, J.; Shenk, R.; Wang, N.; Dasari, R.; Fitzmaurice, M.; Feld, M. Diagnosing breast cancer using Raman spectroscopy: prospective analysis. *Journal of Biomedical Optics*, Vol 14 (5), 2009, pp 054023.

[11] Nguyen, F.; Zysk, A.; Chaney, E.; Kotynek, J.; Oliphant, U.; Bellafiore, F.; Rowland, K.; Johnson, P.; Boppart, S. Intraoperative evaluation of breast tumor margins with optical coherence tomography. *Cancer Research*, Vol 69 (22), 2009, pp 8790–8796.

[12] Fitzgerald, A.; Wallace, V.; Jimenez-Linan, M.; Bobrow, L.; Pye, R.; Purushotham, A.; Arnone, D. Terahertz pulsed imaging of human breast tumors. *Radiology*, Vol 239 (2), 2006, pp 533-540.

[13] Johnson, K.; Sarma, D.; Hwang, E. Lobular breast cancer series: imaging. *Breast Cancer Research*, Vol 17, 2015, pp 94.

[14] Brem, R.; Ioffe, M.; Rapelyea, J.; Yost, K.; Weigert, J.; Bertrand, M.; Stern, L. Invasive lobular carcinoma: Detection with mammography, sonography, MRI, and breast-specific gamma imaging. *American Journal of Roentgenology*, Vol 192, 2009, pp 379-383.

[15] Sakr, R.; Poulet, B.; Kaufman, G.; Nos, C.; Clough, K. Clear margins for invasive lobular carcinoma: a surgical challenge. *European Journal of Surgical Oncology*, Vol 37, 2011, pp 350-356.

[16] Doyle, T.; Tew, A.; Warnick, K.; Carruth, B. Simulation of elastic wave scattering in cells and tissues at the microscopic level. *Journal of the Acoustical Society of America*, Vol 125 (3), 2009, pp 1751-1767.

[17] Huang, S.; Li, P. Ultrasonic computed tomography reconstruction of the attenuation coefficient using a linear array. *IEEE Transactions on Ultrasonics, Ferroelectrics, and Frequency Control*, Vol 52 (11), 2005, pp 2011-2022.

[18] Jeong, J.; Shin, D.; Do, S.; Blanco, C.; Klipfel, N.; Holmes, D.; Hovanessian-Larsen, L.; Marmarelis, V. Differentiation of cancerous lesions in excised human breast specimens using multiband attenuation profiles from ultrasonic transmission tomography," *Journal of Ultrasound in Medicine*, Vol 27, 2008, pp 435-451.

[19] Oelze, M.; Zachary, J. Examination of cancer in mouse models using high-frequency quantitative ultrasound. *Ultrasound in Medicine and Biology*, Vol 32 (11), 2006, pp 1639-1648.

[20] Doyle, T.; Patel, H.; Goodrich, J.; Kwon, S.; Ambrose, B.; Pearson, L. Ultrasonic differentiation of normal versus malignant breast epithelial cells in monolayer cultures. *Journal of the Acoustical Society of America*, Vol 128 (5), 2010, pp EL229-EL235.

[21] Bruno, I.; Kumon, R.; Heartwell, B.; Maeva, E.; Maev, R. *Ex vivo* breast tissue imaging and characterization using acoustic microscopy**.** *Acoustical Imaging*, *Volume 28*, M. P. André, Springer, Dordrecht (Netherlands), 2007.

[22] Banihashemi, R.; Vlad, R.; Debeljevic, B.; Giles, A.; Kolios, M.; Czarnota, G. Ultrasound imaging of apoptosis in tumor response: Novel preclinical monitoring of photodynamic therapy effects. *Cancer Research*, Vol 68 (20), 2008, pp 8590-8596.

[23] Vlad, R.; Kolios, M.; Moseley, J.; Czarnota, G.; Brock, K. Evaluating the extent of cell death in 3D high frequency ultrasound by registration with whole-mount tumor histopathology. *Medical Physics*, Vol 37 (8), 2010, pp 4288-4297.

[24] Doyle, T.; Factor, R.; Ellefson, C.; Sorensen, K.; Ambrose, B.; Goodrich, J.; Hart, V.; Jensen, S.; Patel, H.; Neumayer, L. High-frequency ultrasound for intraoperative margin assessments in breast conservation surgery: a feasibility study. *BMC Cancer*, Vol 11, 2011, pp 444.

[25] Culjat, M.; Goldenberg, D.; Tewari, P.; Singh, R. A review of tissue substitutes for ultrasound imaging. *Ultrasound in Medicine and Biology*, Vol 36, 2010, pp 861-873.